

## Magnetic susceptibility of Cs and Rb from the vapor to the liquid phase

Ronald Redmer\* and William W. Warren, Jr.

*Department of Physics, Oregon State University, Weniger Hall 301, Corvallis, Oregon 97331-6507*

(Received 30 April 1993)

We apply the model of a partially ionized gas to calculate the electronic magnetic susceptibility of Cs and Rb vapor along the coexistence curve. The deviations from the Curie law as obtained in the experiments of Freyland [Phys. Rev. B **20**, 5104 (1979) and J. Phys. (Paris) Colloq. **41**, C8-74 (1980)] are due to the formation of spin paired dimers. The enhancement of the electronic magnetic susceptibility at about 2–3 times the critical density in the domain of the expanded liquid can be explained by the formation of higher clusters such as  $\text{Cs}_2^+$  and  $\text{Rb}_2^+$ . The implications on the mechanism of the metal-nonmetal transition in expanded liquid metals are discussed.

### I. INTRODUCTION

A metal-nonmetal transition occurs in fluid metals when they are thermally expanded from the melting point up to supercritical conditions. Measurements of the electrical conductivity  $\sigma$ ,<sup>1–3</sup> the equation of state  $p(\rho, T)$ ,<sup>4,5</sup> the thermopower  $\alpha$ ,<sup>6,7</sup> the static<sup>8</sup> and dynamic<sup>9</sup> structure factor  $S(q)$  and  $S(q, \omega)$ , respectively, the optical reflectivity, and the dielectric function<sup>10</sup> have been performed for Hg and/or alkali metals. The pronounced changes of these quantities near the critical point of the liquid-gas phase transition imply that there the electronic and structural properties also undergo significant changes and that a metal-nonmetal transition takes place when the critical point is approached.

The coincidence of two instability mechanisms, the ordinary liquid-gas phase instability and the metal-nonmetal transition, leads to some peculiarities in the behavior of expanded fluid metals compared with that of nonconducting fluids. First, and most evident, the electrical conductivity shows a sharp decrease in a narrow density range near the critical point from values of  $\sigma > 10^3 \Omega^{-1} \text{cm}^{-1}$ , characteristic of the degenerate electron gas in metals, to values less than  $\sigma \leq 10^2 \Omega^{-1} \text{cm}^{-1}$ . This value, the minimum metallic conductivity as estimated by Mott, is conventionally used to locate the metal-nonmetal transition at finite temperatures. In the vapor, the conductivity decreases further when leaving the coexistence line and behaves like that of a weakly ionized gas as found recently for Cs.<sup>5</sup>

The thermopower can change its sign near the critical point as found for Hg.<sup>7</sup> The interesting question arises, whether or not such a behavior is typical for expanded fluid metals near the metal-nonmetal transition.

Second, the coexistence curve of Hg and the alkali metals in reduced units ( $\rho/\rho_c$  versus  $T/T_c$ ) shows a strong asymmetry relative to that of nonconducting fluids such as the inert gases.<sup>4,5</sup> There is clearly no common law of corresponding states for both the liquid metals and the inert gases, and even not for the liquid metals as one group. However, the alkali metals behave very similarly to each other and there is a systematic trend to the

behavior of that of nonconducting fluids with increasing ionization energy from Cs to Li.

Third, the dielectric properties of Hg as derived from the reflectivity data<sup>10</sup> indicate a strong influence of critical fluctuations near the critical point. As a result, a huge dielectric anomaly is obtained compared to that of nonconducting fluids.

All these experimental data give no complete insight into the nature of this metal-nonmetal transition. The *magnetic properties* such as the susceptibility  $\chi(\mathbf{q}, \omega)$  of Cs and Rb,<sup>11,12</sup> of Na,<sup>13</sup> and Li (Ref. 14, see also Ref. 15), or the Knight shift  $K$  (Refs. 16 and 17) as function of density  $\rho$  and temperature  $T$  are more sensitive with respect to the interactions in these systems. Generally, many-particle theories are needed to explain the behavior of these quantities.<sup>18</sup>

The volume electronic susceptibility extracted from Freyland's measurements<sup>11,12</sup> of the mass susceptibility along the coexistence curve of Cs and Rb exhibits an interesting behavior. We have displayed the Cs data in Fig. 1 (see also Ref. 17). At the melting point, the electronic susceptibility is enhanced by a factor of 1.6–2.2 compared to the Pauli spin susceptibility of a free-electron gas which is typical for metals.

In the past decade satisfactory calculations have been performed of the ground-state energy, the spin susceptibility, and of the static pair correlation function for the strong-coupling regime,  $2 \leq r_s \leq 5.65$ , which matches the conditions of the degenerate electron gas near the melting point of simple metals.<sup>19</sup> The enhancement of the spin susceptibility derives from the local-field corrections to the dynamic dielectric function  $\epsilon(\mathbf{q}, \omega)$  and from the effective electron mass  $m^*$  which is described by the conventional Stoner model. These quantities are not directly measurable and there is still a great variation in the theoretical results for the susceptibility.

This situation becomes much more complex for expanded liquid metals, since we have to deal with coupling strengths of  $5 \leq r_s \leq 15$ , a gradual transition to nondegenerate conditions, and thermal excitations near the critical point. When the density of fluid Cs is lowered by thermal expansion, the electronic susceptibility first decreases and

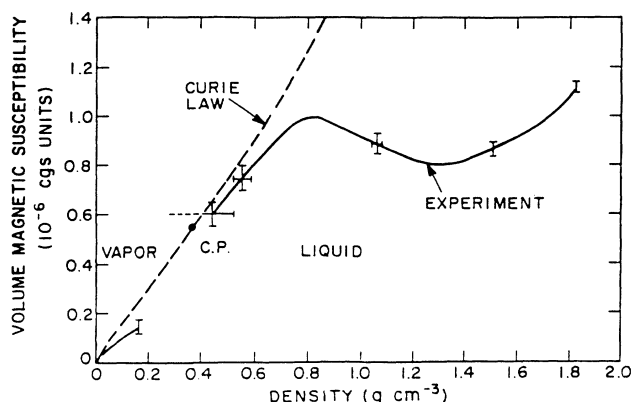


FIG. 1. Spin susceptibility (per unit volume) vs density along liquid-gas coexistence curve of Cs extracted from Freyland's measurements (Ref. 11) by Warren, Brennert, and El-Hanany (Ref. 17). Dashed line indicates Curie law for one electron per atom.

reaches a minimum value at three times the critical density where the enhancement factor is about unity. The electronic susceptibility is enhanced again for lower densities and reaches its maximum value at about twice the critical density, where the enhancement factor is nearly two. For densities below this point, a strong decrease is obtained. However, the data provide a systematic deviation from the Curie law even at vapor densities.

This behavior together with that of the nuclear spin-lattice relaxation rate  $1/T_1$  and of the charge density at the nucleus,  $\langle |\Psi(0)|^2 \rangle$ , which are derived from both the susceptibility and Knight-shift measurements,<sup>17</sup> are not explainable by an extension of the conventional Stoner model to these conditions.

Various aspects of this metal-nonmetal transition have been studied on the basis of existing theories.<sup>20</sup> The Hubbard model treats electron correlation effects in crystalline materials. Assuming that a band structure concept is applicable up to the critical region of fluid metals, the metal-nonmetal transition can be explained by a splitting of the conduction band into two Hubbard bands caused by the intra-atomic electron-electron interaction at reduced densities. Thus, the transport should be thermally activated as in semiconductors.

A correlation enhancement of both the spin susceptibility and the electronic specific heat is expected from the calculation of Brinkman and Rice.<sup>21</sup> The possibility of a ferromagnetic ground-state for expanded liquid metals as inherent in the Stoner model is avoided due to the derivation of a reduced degeneracy temperature so that the susceptibility saturates at the Curie value for elevated temperatures.

The liquid state is disordered and has only locally an ordered structure. We know from neutron scattering experiments<sup>8,9</sup> that the thermal expansion of Cs and Rb leads to an almost linear decrease of the coordination number rather than to an increased near-neighbor distance. This feature has been used as a basis for electronic structure calculations for expanded liquid metals within

the one-electron (band) theory. One-electron theory has been highly successful in explaining the electronic properties of simple metals at solid-state densities. The liquid metal at lower densities is modeled by assuming various crystal structures with different coordination numbers but fixed near-neighbor distance.<sup>22,23</sup> In addition, the effects of changing the interatomic separation for a given structure can be studied.<sup>23</sup> In these calculations, *antiferromagnetic* ordering seems to be the favored ground state for the alkali metals rather than a ferromagnetic one, similar to the behavior of H.<sup>24</sup> These one-electron band-structure calculations fail completely in explaining the behavior of the Korringa relation and of the charge density at the nucleus.

Focusing on the effects of disorder, one has to deal with the phenomenon of Anderson localization<sup>25</sup> and a subsequent disorder-induced metal-nonmetal transition. In fluid metals, a pseudogap of the density of states might develop at the Fermi level during the expansion and the states around  $E_F$  become localized.<sup>20</sup> We have seen that the one-electron picture is not sufficient for the description of the electron structure during the metal-nonmetal transition and that electron correlation effects play an important role. Logan<sup>26</sup> studied the effects of both electron correlation (on Hartree-Fock level) and of disorder (given by a random distribution of all sites which is characterized by a classical pair potential) in a disordered Hubbard model. The introduction of localized magnetic moments as a first effect of electron correlation and a simple scheme for averaging over all distributions of the sites leads to the distinction of three density domains: a nonmagnetic metallic state at high densities, a metallic state with local magnetic moments at intermediate densities, and a nonmetallic state with magnetic moments at low densities. Here, at least a qualitative agreement with the experimentally observed behavior of the magnetic susceptibility and of the electrical conductivity is achieved for expanded liquid alkali metals.

A completely different approach to these systems does not utilize methods of solid-state physics which are clearly applicable for the high-density metal, but starts with the low-density vapor. For supercritical temperatures,  $T \gg T_c$ , a dense plasma state is reached which can be treated by consistent quantum statistical methods (for reviews, see Refs. 27–30). The effects of dynamic screening and self-energy, of arbitrary degeneracy, of the Pauli exclusion principle, of structure factor and two-particle nonequilibrium correlations have been studied for the thermodynamic, transport, and optical properties of those strongly coupled plasmas.

A special effect in low-temperature plasmas, i.e., for temperatures around  $T_c$  as considered here, is the formation of neutral and charged clusters such as atoms  $A$ , dimers  $A_2$ , and molecular ions  $A_2^+$  or  $A^-$  out of the elementary particles electrons  $e$  and ions  $A^+$  so that the plasma becomes partially ionized. The correlations between the particles lead to an opposite effect, the decrease of the bound-state energies with increasing density, which is known as the lowering of the ionization energy for the case of atoms. At densities high enough to let even the deepest energy level merge into the continuum of

scattering states, the plasma becomes fully ionized, and a corresponding nonmetal-to-metal-like transition takes place in a relatively narrow density region. The question whether or not this so-called plasma-phase transition has a real phase instability with a second critical point has been the focus of intense work done for hydrogen and inert gas plasma (see Refs. 31–33).

Contrary to hydrogen and the inert gases, where this metal-nonmetal transition takes place at plasma conditions well separated from the ordinary liquid-gas phase transition, in the expanded liquid alkali metals and in Hg both transitions are superposed due to the relatively low ionization potentials in these materials. The model of a partially ionized plasma has been successfully applied to calculate the equation of state<sup>34,35</sup> and the transport properties<sup>36,37</sup> for the density-temperature region near the critical point of Cs. A relatively good agreement with the experimental values was found for the critical temperature of all alkali metals. The sharp decrease of the electrical conductivity near the critical point cannot be explained by any extension of the nearly free electron model but by the formation of neutral atoms and dimers. This mechanism also leads to the change in sign for the thermopower.<sup>38</sup>

We will utilize this approach to calculate the magnetic susceptibility of Cs and Rb along the liquid-vapor coexistence line and compare with the experimental results of Freyland.<sup>11,12</sup> These experiments indicated not only susceptibility enhancement at expanded liquid densities, but also strong deviations from the Curie law at vapor densities. First, we will focus our attention on the possible mechanism which causes this special behavior, the formation of spin-paired dimers. The concept of particle clustering is then generalized to allow for higher-order clusters such as molecular ions  $\text{Cs}_2^+$  and  $\text{Rb}_2^+$  so that even higher densities can be treated, especially the region up to two or three times the critical density. For higher densities, the fully ionized state is approached and the conventional Stoner model for the magnetic susceptibility yields the limiting behavior for this metallic state.

The thermodynamic and transport properties of alkali-metal plasmas were also calculated by Alekseev and Iakubov<sup>39</sup> within the model of a weakly ionized gas. Hernandez<sup>40</sup> later adopted this point of view and found consistent results for the thermodynamic and electric properties up to the critical region. Both approaches considered the chemical equilibria between various polyatomic species and found evidence for the occurrence of higher clusters in that domain. We compare with these earlier works after describing our approach in detail.

Our paper is organized as follows. In Sec. II we outline the basic theoretical approach to the composition and the thermodynamic functions of a strongly coupled plasma, and give the respective results for Cs and Rb. The results available so far for the contributions of various species to the total magnetic susceptibility are critically reviewed in Sec. III. In Sec. IV we present our findings for the magnetic susceptibility of Cs and Rb and compare with the experimental values and previous calculations. In Sec. V we give a brief summary of principal results and conclusions.

## II. EQUATION OF STATE FOR PARTIALLY IONIZED PLASMAS

In this section we give a short review of the quantum statistical approach to the equation of state (EOS) and the composition of dense and partially ionized plasmas. Besides the derivation of the basic expressions for the thermodynamic functions which are capable of taking into account interaction effects systematically, we explain the approximate evaluation of these formulae for alkali-metal plasmas.

### A. Short review of the theoretical approach

In order to construct systematic approximations for the EOS, a diagram representation for the Green's functions can be applied. The starting point is the relation between the number density as a function of the temperature and chemical potential,  $n_c = n_c(\beta, \mu_c)$ , and the imaginary part of the Green's function—the spectral function,<sup>41</sup>

$$n_c(\beta, \mu_c) = \frac{1}{\Omega_0} \sum_{\mathbf{k}} \int \frac{d\omega}{\pi} f_c(\omega) \text{Im} G_c(\mathbf{k}, \omega - i0^+), \quad (1)$$

where  $\beta = 1/(k_B T)$  is the inverse temperature,  $\Omega_0$  the normalization volume, and  $\mu_c$  denotes the chemical potential of species  $c = e, A^+$ .  $f_c(E) = \{\exp[\beta(E - \mu_c)] + 1\}^{-1}$  is the Fermi function. The chemical potential  $\mu(\beta, n)$  is obtained from Eq. (1) by inversion, whereas the pressure  $p(\beta, \mu) = \int_{-\infty}^{\mu} d\bar{\mu} n(\beta, \bar{\mu})$  follows after a simple integration.

The Green's function is given by the Dyson equation,

$$\frac{1}{G_c(\mathbf{k}, z)} = \hbar z - E_c(k) - \Sigma_c(\mathbf{k}, z), \quad (2)$$

which also defines the self-energy  $\Sigma_c(\mathbf{k}, z)$ .  $E_c(k) = \hbar^2 k^2 / (2m_c)$  is the kinetic energy of free particles. Quasiparticle energies are usually defined by the solution of

$$\epsilon_c(\mathbf{k}) = E_c(k) + \text{Re} \Sigma_c[\mathbf{k}, \epsilon_c(k) / \hbar + i0]. \quad (3)$$

The simplest case corresponds to  $\Sigma_c = 0$ , and from Eqs. (1) and (2) we get the EOS for an ideal gas,  $n_c^{id}(\beta, \mu_c) = (1/\Omega_0) \sum_{\mathbf{k}} f_c[E_c(k)]$ . First-order perturbation theory leads to a Hartree-Fock shift  $\Sigma_c^{\text{HF}}(k) = \Delta^{\text{HF}}(k)$  and we have  $n_c^{\text{HF}}(\beta, \mu_c) = 1/\Omega_0 \sum_{\mathbf{k}} f_c[E_c(k) + \Delta^{\text{HF}}(k)]$ .

In order to describe the formation of atoms  $A$  out of the elementary species electrons  $e$  and ions  $A^+$ , as well as of higher-order clusters such as dimers  $A_2$  or molecular ions  $A_2^+$ ,  $A^-$ , the self-energy and also the polarization function  $\Pi(\mathbf{q}, \omega)$  have to be decomposed into a sum over the contributions for  $N$ -particle ladder  $T$  matrices (for details, see Refs. 34 and 35). These quantities are determined by respective Bethe-Salpeter equations with an effective two-particle interaction kernel  $V_{cd}^{(2, \text{eff})}$  that contains the dynamically screened potential and further in-medium corrections to their energy spectrum via the cluster contributions to the polarization function. We consider here the dominant bound state part of the  $N$ -

particle  $T$  matrices with  $N \geq 3$ . For atoms ( $N=2$ ), the scattering state part may become of importance.

Then inserting this cluster expansion into the EOS (1), the total density of, e.g., electrons  $c=e$  is given by

$$n_e(\beta, \mu_e) = n_e^0 + n_e^{(2, \text{corr})} + n_{A_2^+}^{(3)} + 2n_{A_2}^{(4)} + \dots, \quad (4)$$

where the partial density of a  $N$ -particle cluster,  $n^{(N)}$  with  $N \geq 3$ , is given by its partition function

$$n^{(N)} = \frac{1}{\Omega_0} \sum_{\nu, \mathbf{P}}^{(b)} \{ \exp[-\beta(\varepsilon_{\nu, \mathbf{P}}^{(N)} - \mu_1 - \mu_2 - \dots - \mu_N)] + (-1)^{N-1} \}^{-1}. \quad (5)$$

$\nu$  is the set of internal quantum numbers and  $\mathbf{P}$  is the total momentum of the  $N$ -particle cluster. The energy eigenvalues  $\varepsilon_{\nu, \mathbf{P}}^{(N)}$  and wave functions  $\Psi_{\nu, \mathbf{P}}^{(N)}$  are solutions of the  $N$ -particle Bethe-Salpeter equations and are related to those for the isolated  $N$ -particle cluster  $E_{\nu, \mathbf{P}}^{(N)}$  and  $\Psi_{\nu, \mathbf{P}}^{(N, 0)}$  by

$$n_c^0 = \frac{1}{\Omega_0} \sum_{\mathbf{k}} f_c[\varepsilon_c(k)], \quad \varepsilon_c(k) = E_c(k) + \Delta_c, \quad (7)$$

$$\Delta_c = \left\{ \frac{1}{\Omega_0} \sum_{\mathbf{k}} f'_c[\varepsilon_c(k)] \text{Re} \Sigma_c[\mathbf{k}, \varepsilon_c(k) + i0] \right\} / \left\{ \frac{1}{\Omega_0} \sum_{\mathbf{k}} f'_c[\varepsilon_c(k)] \right\},$$

and utilizing the optical theorem, a generalized Beth-Uhlenbeck formula<sup>47</sup> was derived for the correlated density

$$n_c^{(2, \text{corr})} = \frac{1}{\Omega_0} \sum_{q, d, l} (2l+1) \left[ 1 - \frac{(-1)^l}{2} \delta_{cd} \right] \times \left\{ \sum_n g_{cd} \left[ \varepsilon_{nl} + \frac{\hbar^2 \mathbf{q}^2}{2M_{cd}} + \Delta_c + \Delta_d \right] + \int_0^\infty dk g_{cd} \left[ \frac{\hbar^2 \mathbf{k}^2}{2\mu_{cd}} + \frac{\hbar^2 \mathbf{q}^2}{2M_{cd}} + \Delta_c + \Delta_d \right] \frac{1}{\pi} \frac{d\delta_l(k)}{dk} 2 \sin^2 \delta_l(k) \right\}. \quad (8)$$

$M_{cd}$  and  $\mu_{cd}$  denote the total and reduced mass of a pair of particles ( $c, d$ ), respectively and  $g_{cd}(E) = \{ \exp[\beta(E - \mu_c - \mu_d)] - 1 \}^{-1}$  is the Bose function for two-particle states.

The correlated density consists of the sum over the discrete bound state energies  $\varepsilon_{nl}$  and the integral over the continuous scattering states, characterized by their scattering phase shifts  $\delta_l(k)$ . Zimmermann and Stolz<sup>46</sup> pointed out that the difference to the standard Beth-Uhlenbeck formula, the additional factor  $2 \sin^2 \delta_l(k)$  in the scattering state part, is a result of putting as much correlation as possible into the definition of the quasiparticle density  $n_c^0$  via the full self-energy shift  $\Delta_c$ .

They demonstrated the well-known compensation of discontinuities in the bound state part which occur whenever a bound state disappears due to self-energy and screening effects. The respective contributions are taken over by the scattering state part and the whole partition function, Eq. (8), remains a smooth function.

For the nondegenerate case, Bose and Fermi functions can be replaced by Boltzmann factors. Restricting to that contribution  $d \neq c$  which is capable of forming bound states, Eq. (8) can be used for the derivation of a mass ac-

$$\varepsilon_{\nu, \mathbf{P}}^{(N)} = E_{\nu, \mathbf{P}}^{(N)} + \Delta E_{\nu, \mathbf{P}}^{(N)}, \quad (6)$$

$$\Delta E_{\nu, \mathbf{P}}^{(N)} = \sum_{i < j}^N \langle \Psi_{\nu, \mathbf{P}}^{(N, 0)} | V_{ij}^{(2, \text{eff})} - V_{ij} | \Psi_{\nu, \mathbf{P}}^{(N, 0)} \rangle.$$

The simplest case, the formation of atoms  $A$  out of electrons  $e$  and ions  $A^+$  was explained by Stolz and Zimmermann<sup>42</sup> within a quasiparticle approach to the spectral function of single particles and by applying a  $T$ -matrix approximation for the self-energy. A consistent expansion of the spectral function with respect to the imaginary part of the self-energy was carried out by Kremp *et al.*<sup>43</sup> and an EOS for quasiparticles was derived which takes into account correlation effects in a genuine way. This EOS has been solved for nuclear matter<sup>44</sup> and ionic plasmas.<sup>34, 35, 45</sup>

Zimmerman and Stolz<sup>46</sup> improved this approach by deriving an EOS (1) which is the sum of the density of free quasiparticles,  $n_c^0$ , and of a density of correlated two-particle states,  $n_c^{(2, \text{corr})}$ . Replacing the slightly  $\mathbf{k}$ -dependent self-energy shift in Eq. (3) by a constant quantity  $\Delta_c$  which is fixed by the free quasiparticle density,

tion law  $e + A^+ \rightleftharpoons A$  and a respective ionization degree  $\alpha$  according to,<sup>46</sup>

$$\alpha = n_c^0 / [n_c^0 + n_c^{(2, \text{corr})}],$$

$$n_c^0 = 2\Lambda_c^{-3} \exp[-\beta(\Delta_c - \mu_c)],$$

$$n_c^{(2, \text{corr})} = n_c^0 n_d^0 \Lambda_{cd}^3 Z_{cd}^{(b)}, \quad (9)$$

$$Z_{cd}^{(b)} = \sum_l (2l+1) \sum_n \{ \exp(-\beta \varepsilon_{nl}) - 1 + \beta \varepsilon_{nl} \}.$$

$\Lambda_c = (2\pi\beta\hbar^2/m_c)^{1/2}$  is the thermal wavelength. The use of higher-order Levinson theorems<sup>48</sup> projects the first expansion terms of the bound-state part with respect to  $\beta \varepsilon_{nl}$  into the scattering state part. In this way, the finite Planck-Larkin partition function for the bound state part,  $Z_{eA^+}^{(b)}$ , can be derived in a natural way<sup>49</sup> and has not to be introduced *ad hoc* in order to avoid its divergence for low densities. The bound-state part dominates the partition function of alkali-metal atoms for low temperatures considered here so that the scattering state part can be neglected. This may change when considering the related nonmetal-to-metal transition in hydrogen or the inert gas plasmas where the temperatures are much higher.

Reactions between polyatomic species in a dense alkali plasma were treated within the given approach in an earlier paper<sup>35</sup> up to the region near the critical point. Good agreement with the measured values (deviations less than 10%) was found for the critical temperatures of Na–Cs. The critical densities and pressures, however, differ from the experimental results up to a factor of 5 which indicates the necessity of including further effects in this region.

Similar approaches were already used by Alekseev and Iakubov<sup>39</sup> and Hernandez<sup>40</sup> for dense alkali plasma and fluids who also found a strong influence of higher clusters on the thermodynamic as well as transport properties. They used relatively simple models for the interaction corrections to the thermodynamic functions such as the Debye-Hückel and the Thomas-Fermi theory, or the concept of excluded volume, but still obtained reasonable results.

We will utilize here the more general expressions for the partial densities and the quasiparticle shifts derived in the previous section. We take into account the interactions between *all* species, especially those between charged and neutral particles (polarization) and between neutrals (van der Waals attraction and hard-core repulsion). We restrict our calculations to the formation of dimers,  $2A \rightleftharpoons A_2$ , and of molecular ions,  $A^+ + A \rightleftharpoons A_2^+$ , which can be described by respective mass action laws,

$$n_{A_2}^{(4)} = [n_e^{(2, \text{corr})}]^2 K_{A_2}, \quad n_{A_2^+}^{(3)} = n_e^{(2, \text{corr})} n_{A^+} K_{A_2^+}. \quad (10)$$

The quantities  $K$  are given by the partition functions of the species involved in the reaction and reduce to the well-known Saha equations only in the low-density limit. For arbitrary densities, we have to consider the self-energy corrections to the one-, two-, and  $N$ -particle states as well as the change of the energy spectrum of the clusters via the density corrections (dynamic screening, Pauli exclusion principle, etc.) to the  $N$ -particle Bethe-Salpeter equations, so that the  $K$ 's become dependent on density and temperature. We will give explicit expressions for that in the next subsection. Higher neutral and charged clusters are of less importance along the liquid-vapor coexistence curve of Cs and Rb as estimated from the respective (ideal) Saha equations.

Due to the condition of charge neutrality, the different mass action laws are not independent from each other and we have finally a coupled, strongly nonlinear system of equations,

$$[n_e^0]^2 \Lambda_{eA}^3 + Z_{eA}^{(b)+} = n_e^{(2, \text{corr})} \{1 + n_e^{(2, \text{corr})} K_{A_2^+}\}. \quad (11)$$

### B. Quasiparticle shifts and partition functions

We will solve the mass action laws, Eqs. (9) and (11), by inserting appropriate expressions for the quasiparticle shifts and the partition functions for atoms, dimers, and molecular ions which were derived earlier. The shifts  $\Delta_c$  can be decomposed into the Hartree-Fock (HF) and Montroll-Ward (MW) contributions, characterizing the self-energy of charged particle interactions in second order with respect to the Coulomb potential

$V(q) = e^2 / (\epsilon_0 q^2)$ , and a polarization contribution (PP) which is due to interactions between the charged particles and the neutral bound states,

$$\Delta_c = \Delta_c^{\text{HF}} + \Delta_c^{\text{MW}} + \Delta_c^{\text{PP}}. \quad (12)$$

For simplicity, we have used the Padé approximations of Ebeling and Richert<sup>50</sup> for the charged particle self-energy in alkali plasmas,  $\Delta_c^{\text{HF}} + \Delta_c^{\text{MW}}$ , which interpolate between the known limiting cases of nondegeneracy (Debye-Hückel theory), the strong-coupling limit for the electrons (Gell-Mann and Brueckner result<sup>51</sup>), and the case of strongly correlated ions. Thus, these formulas cover the whole density region from the plasma to the liquid state in which we are interested in within an estimated error of about 20% (Ref. 52).

The polarization contribution  $\Delta_c^{\text{PP}}$  was calculated via the quantum defect method for arbitrary densities for the interaction of electrons with all alkali-metal atoms.<sup>53</sup> The results can be given in a parametrized form as linearized virial coefficients  $B_{c,A}^{\text{PP}}$  with respect to a local polarization potential  $V^{\text{PP}}(R)$  (see Ref. 34),

$$\begin{aligned} \Delta_c^{\text{PP}} &= n_A B_{c,A}^{\text{PP}}, \\ B_{c,A}^{\text{PP}} &= \int d\mathbf{R} V^{\text{PP}}(R), \\ V^{\text{PP}}(R) &= -\frac{e^2 \alpha_D \exp(-2\kappa R)}{2(4\pi\epsilon_0)^2 (R^2 + r_0^2)^2} (1 + \kappa R)^2. \end{aligned} \quad (13)$$

The dipole polarizability  $\alpha_D$  and the cutoff radius  $r_0$  were calculated in Refs. 35 and 53.  $\kappa = (\beta e^2 n_e^0 / \epsilon_0)^{1/2}$  is the inverse screening length.

The shift of the energy spectrum of atoms,  $\Delta E_{n,\mathbf{P}}^{(2)}$ , is due to the interaction with free quasiparticles (PP) as well as with other atoms and clusters (vdW, HC), and can be derived from the different in-medium corrections to the Bethe-Salpeter equation (see Refs. 34, 35, and 53),

$$\Delta E_{n,\mathbf{P}}^{(2)} = \Delta E_{n,\mathbf{P}}^{\text{PP}} + \Delta E_{n,\mathbf{P}}^{\text{vdW}} + \Delta E_{n,\mathbf{P}}^{\text{HC}}. \quad (14)$$

The polarization contribution is given by  $\Delta E_{n,\mathbf{P}}^{\text{PP}} = n_c^{(2, \text{corr})} B_{c,A}^{\text{PP}}$  similar to Eq. (13). The second one describes the long-range van der Waals attraction between atoms and was calculated by means of the quantum defect method again,<sup>54</sup>  $\Delta E_{n,\mathbf{P}}^{\text{vdW}} = n_c^{(2, \text{corr})} B_{A,A}^{\text{vdW}}$ . The last contribution is due to the short-range hard-core repulsion between clusters. This contribution was treated by utilizing the modified Carnahan-Starling expression derived by Mansoori *et al.*<sup>55</sup> for the chemical potential of a mixture of hard spheres,  $\Delta E_{n,\mathbf{P}}^{\text{HC}} = \mu_{A,A}^{\text{HC}}$ .

The mass action laws for the dimers and molecular ions, Eqs. (10), require expressions for the partition functions  $K_{A_2}$  and  $K_{A_2^+}$ . We treat these quantities in the usual way by separating the internal quantum numbers  $\{\nu, \mathbf{P}\}$  with respect to the translational, spin, electronic, rotational, and vibrational degrees of freedom,

$$\frac{1}{\Omega_0} \sum_{\nu, \mathbf{P}}^{(b)} g(\epsilon_{\nu, \mathbf{P}}^{(N)}) = \Lambda_{A_N}^{-3} \sigma_{A_N}^{\text{spin}} \sigma_{A_N}^{\text{el}} \sigma_{A_N}^{\text{rot}} \sigma_{A_N}^{\text{vib}}. \quad (15)$$

These different contributions are given by<sup>56</sup>

$$\begin{aligned}\sigma_{A_N}^{\text{rot}} &= \beta hc / B_{A_N}, \\ \sigma_{A_N}^{\text{vib}} &= \left[ 1 - \exp \left( -\frac{\omega_{A_N}}{\beta hc} \right) \right]^{-1}, \\ \sigma_{A_N}^{\text{el}} &= \exp(\beta D_{A_N} + \Delta E_{A_N}),\end{aligned}\quad (16)$$

where  $B_{A_N}$ ,  $\omega_{A_N}$ , and  $D_{A_N}$  are the characteristic rotational constant, the vibrational frequency, and the dissociation energy of the cluster  $A_N$ , respectively.  $c$  is the speed of light.

We have taken into account interaction corrections to these mass action laws via the quantity  $\Delta E_{A_N}$ . Comparing the dipole polarizabilities of alkali-metal atoms and dimers,<sup>57</sup>  $f = \alpha_{A_2} / \alpha_A$ , one finds  $f \approx 1.5$ . Applying the London relation<sup>58</sup> for the van der Waals constants,  $C_{A,B} \approx \frac{3}{2} \alpha_A \alpha_B \Delta E_A \Delta E_B / (\Delta E_A + \Delta E_B)$ , and considering the respective resonance energies of the atoms and the dissociation energies of the dimers for  $\Delta E_A$  and  $\Delta E_B$ , the following estimates can be given for the virial coefficients between the higher alkali-metal clusters,

$$\begin{aligned}B_{c,A_2}^{\text{PP}} &\approx 1.5 B_{c,A}^{\text{PP}}, \\ B_{A_2,A}^{\text{vdW}} &\approx 0.45 B_{A,A}^{\text{vdW}}, \\ B_{A_2,A_2}^{\text{vdW}} &\approx 0.4 B_{A,A}^{\text{vdW}}.\end{aligned}\quad (17)$$

Effective hard-core radii for the dimers and molecular ions can be derived from the known atomic and ionic radii and the equilibrium distances in these clusters.

### C. Results for the composition of Cs and Rb

The system of Eqs. (9)–(11) was solved for Cs and Rb. The nonideality corrections to the mass action laws were treated as described above. All the parameters which are necessary for the evaluation of the given formulas are summarized in Table I. We have displayed the composition of Cs and Rb along their liquid-vapor coexistence curves in Figs. 2. For a given temperature, the fractions of the different species were calculated as a function of density. The relevant values are those which match the total density as measured by Jüngst, Knuth, and Hensel.<sup>4</sup>

We can clearly distinguish between three different regions. The first, the low-density vapor, is a weakly ionized gas with an ionization degree of less than 10% and extends up to the critical density. It consists mainly of atoms and dimers, the latter reaching a maximum concentration of about 22%. Even for the lowest densities considered here, a considerable number of dimers was found indicating that the limiting case of an atomic vapor is approached for still lower densities,  $\rho \leq 0.1\rho_c$ .

The second region, from 1 up to 2.5 times the critical density, is characterized by partial ionization. Here all the clusters have strongly varying concentrations which is a result of the nonideality corrections to the mass action laws. Dimers vanish at about 1.5 times the critical density, whereas molecular ions occur only in the narrow range between 1 and 2.5 times the critical density. They reach maximum concentrations of about 38%. The ionization degree is sharply rising with increasing densities which is a result of pressure ionization (Mott effect) as discussed above.

The third region, from 2.5 times the critical density up to the melting point, is fully ionized and completely described by the degenerate electron gas immersed in the positive background of simple alkali-metal ions  $A^+$ .

TABLE I. Parameters necessary for the calculation of the composition of Cs and Rb along the liquid-vapor coexistence curve according to Eq. (9)–(11).

Parameter	Cs	Rb
ionic radius $R_{A^+}$ in $a_B$	3.16	2.78
atomic radius $R_A$ in $a_B$	5.18	4.78
equilibrium distance $d_{A_2^+}$ in $a_B$	9.92 <sup>a</sup>	8.88 <sup>a</sup>
equilibrium distance $d_{A_2}$ in $a_B$	9.0 <sup>a</sup>	7.88 <sup>a</sup>
cutoff radius $r_0$ in $a_B$	4.478 <sup>b</sup>	4.187 <sup>b</sup>
polarizability $\alpha_D$ in $a_B^3$	382.4 <sup>b</sup>	306.0 <sup>b</sup>
$E_{\text{ion}}$ of atoms in eV	4.19	3.89
$E_{\text{diss}}$ of dimers in eV	0.49 <sup>c</sup>	0.40 <sup>c</sup>
$E_{\text{diss}}$ of molecular ions in eV	0.66 <sup>a</sup>	0.72 <sup>a</sup>
rotational constant of dimers $B_{A_2}$ in $\text{cm}^{-1}$	0.0127 <sup>c</sup>	0.0226 <sup>c</sup>
rotational constant of mol. ions $B_{A_2^+}$ in $\text{cm}^{-1}$	0.0092 <sup>a</sup>	0.018 <sup>a</sup>
vibrational frequency of dimers $\omega_{A_2}$ in $\text{cm}^{-1}$	42.019 <sup>c</sup>	57.75 <sup>c</sup>
vibrational frequency of mol. ions $\omega_{A_2^+}$ in $\text{cm}^{-1}$	34.0 <sup>a</sup>	45.0 <sup>a</sup>

<sup>a</sup>Reference 71(c).

<sup>b</sup>Reference 53.

<sup>c</sup>Reference 56.

### III. MAGNETIC SUSCEPTIBILITY OF PARTIALLY IONIZED PLASMAS

#### A. Theoretical model for magnetic susceptibility

The dielectric function  $\epsilon(\mathbf{q}, \omega)$  is given by the retarded density fluctuation correlation function<sup>30,41</sup> and describes the response of the charged particle system to the external longitudinal field as well as the induced density fluctuations. It is more convenient to relate the dielectric function to the associated time ordered correlation function, the polarization function  $\Pi(\mathbf{q}, \omega)$ , via

$$\epsilon(\mathbf{q}, \omega) = 1 - V(q)\Pi(\mathbf{q}, \omega). \quad (18)$$

Besides the self-energy  $\Sigma_c(\mathbf{k}, z)$ , also the polarization function  $\Pi(\mathbf{q}, \omega)$  has to be decomposed with respect to the contributions of  $N$ -particle clusters in systems with bound states,

$$\Pi(\mathbf{q}, \omega) = \Pi^{(1)}(\mathbf{q}, \omega) + \Pi^{(2)}(\mathbf{q}, \omega) + \dots + \Pi^{(N)}(\mathbf{q}, \omega). \quad (19)$$

We will first discuss the contributions of one-particle states,  $\Pi^{(1)}(\mathbf{q}, \omega)$ , to the polarization function. In the

simplest case, this part is given by the random phase approximation (RPA) which neglects correlation effects as well as density fluctuations due to the Coulomb interaction and is valid for the high-density limit,  $r_S \ll 1$ . Considering only the electronic contribution, the Lindhard expression<sup>59</sup> is derived,

$$\Pi_0(\mathbf{q}, \omega) = 2 \sum_{\mathbf{k}} \frac{f_e[\epsilon_e(\mathbf{k})] - f_e[\epsilon_e(\mathbf{k} + \mathbf{q})]}{\hbar\omega + \epsilon_e(\mathbf{k} + \mathbf{q}) - \epsilon_e(\mathbf{k})}. \quad (20)$$

For metallic ( $2 \leq r_S \leq 5.5$ ) and lower densities, correlation effects are important especially at short distances where they prevent the electrons from feeling the full consequences of the induced density fluctuations. These correlations are usually taken into account by introducing the concept of static local-field corrections  $G(q)$ , which have been calculated for a uniform electron gas in various approximations. For recent reviews, see Refs. 19, 27, 60, and 61. The polarization function is then given by

$$\Pi^{(1)}(\mathbf{q}, \omega) = \frac{\Pi_0(\mathbf{q}, \omega)}{1 - G(q)V(q)\Pi_0(\mathbf{q}, \omega)}. \quad (21)$$

In contrast with the spin-symmetric dielectric response to an external field coupling to the (charge) density fluctuations, the response of the electron system to a magnetic field is spin-antisymmetric. The magnetic susceptibility  $\chi(\mathbf{q}, \omega)$  is therefore calculated from the spin-density fluctuation correlation function. The treatment of correlation effects analogous to the dielectric function leads to the following expression:

$$\chi^{(1)}(\mathbf{q}, \omega) = - \frac{\mu_B^2 \Pi_0(\mathbf{q}, \omega)}{1 - G_{as}(q)V(q)\Pi_0(\mathbf{q}, \omega)}, \quad (22)$$

where  $\mu_B$  is the Bohr magneton. For the case of a noninteracting [ $G_{as}(q) = 0$ ] and degenerate electron gas, the Pauli susceptibility follows from Eqs. (20) and (22) in the static and long-wavelength limit,

$$\chi_P^0 = \lim_{\beta\mu_e \rightarrow +\infty} \left\{ \lim_{q \rightarrow 0} \chi^0(\mathbf{q}, \omega = 0) \right\} = \frac{3\mu_B^3 n_e}{2\epsilon_F}, \quad (23)$$

where  $\epsilon_F$  is the Fermi energy and  $n_e$  the free-electron density. Band-structure effects in solid and also liquid metals are usually described by introducing an effective electron mass  $m^*$  in Eq. (23) which leads to a modified expression for the Pauli spin susceptibility in accordance with the Landau theory of Fermi liquids,  $\chi_P = \chi_P^0 m^*/m_e$  (see Ref. 18).

The usual Stoner model for the explanation of the enhancement of the magnetic susceptibility in metals is derived from Eq. (22) by taking into account exchange and correlation effects in form of static local-field corrections  $G_{as}(q)$ , and considering the effective mass of the electrons,  $m^*$ . The Stoner parameter  $\alpha_{ST} = \lim_{q \rightarrow 0} \{ V(q)G_{as}(q)\chi_0(q)m^*/m_e \}$  is about 0.2–0.6 for simple metals at the melting point which yields typical enhancement factors of about 1.25–2.5. As mentioned above, the local-field corrections are not directly measurable and the effective electron mass can be measured only under limited conditions. Thus, the results for

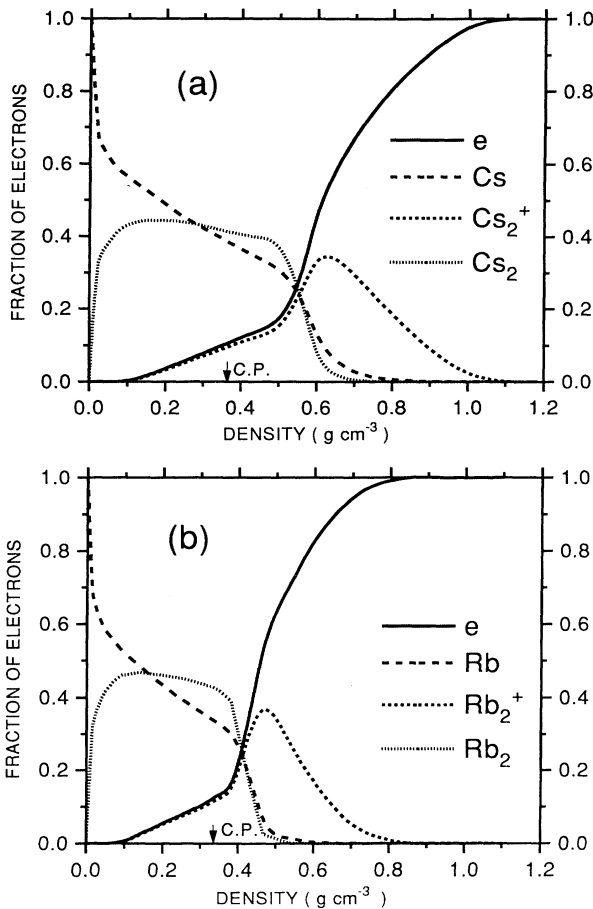


FIG. 2. Composition of Cs (a) and Rb (b) vs density along liquid-gas coexistence curve. Shown is the fraction of free electrons (continuous line) and of electrons localized in atoms (broken line), molecular ions (short broken line), and dimers (short dotted line). Critical points (CP's) are indicated by arrows.

the Stoner parameter depend on the theoretical model applied for their calculation. A summary of a large number of theoretical results was given by Kushida, Murphy, and Hanabusa<sup>60</sup> together with the experimental data available for Li and Na near the melting point.

An additional quantity which can give insight into the behavior of the  $q$ -dependent magnetic susceptibility is the Korringa relation. Expressing the nuclear relaxation rates  $1/T_1$  in terms of the Knight shift  $K$  one finds for the case of noninteracting electrons,

$$\left[ \frac{1}{T_1} \right]_{\text{Korringa}} = \frac{4\pi}{\hbar} \left[ \frac{\gamma_e}{\gamma_n} \right]^2 K^2 k_B T. \quad (24)$$

$\gamma_e$  and  $\gamma_n$  are the gyromagnetic ratios of the electrons and the nuclei, respectively. Utilizing the representation of  $1/T_1$  by the integral over the imaginary part of the susceptibility and of  $K$  by the static, uniform susceptibility, a more general relation can be derived,<sup>17,62</sup>

$$\eta \equiv \left[ \frac{1}{T_1} \right] / \left[ \frac{1}{T_1} \right]_{\text{Korringa}} = \frac{\hbar}{\omega_0} \frac{\int dq q^2 \text{Im}\chi(q, \omega_0)}{2\pi^3 [\text{Re}\chi(0, 0)]^2}, \quad (25)$$

which expresses the relaxation rate relative to the Korringa value for arbitrary densities.  $\omega_0$  is the nuclear resonance frequency. Within the Stoner model, this ratio becomes  $\eta_{\text{ST}} = 1/(2k_F^2) \times \int_0^{2k_F} dq q \{ (1 - \alpha_{\text{ST}}) / [1 - \alpha(q)] \}^2$ , where the  $q$ -dependent Stoner parameter is defined by  $\alpha(q) = V(q)G_{\text{as}}(q)\chi_0(q)m^*/m_e$ . For alkali metals at the melting point,  $\eta_{\text{ST}}$  has typical values of 0.5–0.7. The agreement of both the enhancement factor  $1/(1 - \alpha_{\text{ST}})$  and of the ratio  $\eta_{\text{ST}}$  would be a hint for a consistent model for the susceptibility.<sup>63</sup>

From the behavior of the real and imaginary part of  $\chi(q, \omega)$  within the Stoner model one can conclude that  $\eta$  has to be a decreasing function when expanding the metal along the liquid-vapor coexistence curve. Warren, Brenner, and El-Hanany<sup>17</sup> found the opposite behavior, a strong increase up to values greater than 1, for Cs from their measurements of the Knight shift and the nuclear relaxation rates. This indicates once more the limited validity of the Stoner model.

The next terms in Eq. (19) describe the contributions of  $N$ -particle bound states to the polarization function  $\Pi(\mathbf{q}, \omega)$ . Röpke and Der<sup>64</sup> derived an expression for the dielectric function considering two-particle bound states in addition to the free-particle states,  $\epsilon^{\text{RD}}(\mathbf{q}, \omega) = 1 + V(q)\Pi^{(1)}(\mathbf{q}, \omega) + \Pi^{(2)}(\mathbf{q}, \omega)$ . In the static and long-wavelength limit, this dielectric function can be written as

$$\lim_{q \rightarrow 0} \epsilon^{\text{RD}}(\mathbf{q}, \omega=0) = \frac{A}{q^2} + B + O(q^2). \quad (26)$$

The coefficient  $A$  stems from  $\Pi^{(1)}$  and is connected with the free-particle density via the inverse screening length  $\kappa$ . The quantity  $B$  is derived from  $\Pi^{(2)}$  and shows a Clausius-Mosotti-like behavior via the two-particle density  $n_A^{(2, \text{corr})}$  and their dipole polarizability  $\alpha_D$  according to

$$A = \kappa^2 B, \quad B = 1 + \frac{n_A^{(2, \text{corr})} \alpha_D}{1 - \frac{4\pi}{3} n_A^{(2, \text{corr})} \alpha_D}. \quad (27)$$

We adopt this approach in order to include the bound state contributions to the magnetic susceptibility. Evaluating the respective diagrams, one finds a Curie-like behavior for the localized spins of two-particle bound states (atoms  $A$ ) in the static and long-wavelength limit

$$\chi_C = \lim_{\beta\mu_e \rightarrow -\infty} \{ \lim_{q \rightarrow 0} \chi^{(2)}(\mathbf{q}, \omega=0) \} = \frac{\mu_B^2 n_A}{k_B T}. \quad (28)$$

Generalizing this result for the higher clusters with  $N \geq 3$ , molecular ions  $A_2^+$  with one localized spin yields a Curie-like contribution, Eq. (28), proportional to their partial density  $n_{A_2^+}$ . Dimers  $A_2$  have paired spins and thus no Curie-like paramagnetic contribution.

All bound states have diamagnetic contributions due to orbital magnetization. The respective molar susceptibilities are given by the expectation value  $\langle \mathbf{r}^2 \rangle$  of their wave functions,

$$\chi_{\text{mol}}^{A_N} = - \frac{e^2 L}{6m_e c^2} \langle \mathbf{r}^2 \rangle_{A_N}, \quad (29)$$

where  $L$  is Avogadro's number. Considering the relations between the volume susceptibility  $\chi_V$ , the mass susceptibility  $\chi_g$ , and the molar susceptibility  $\chi_{\text{mol}}$ ,

$$\chi_V = \rho \chi_g, \quad \chi_g = \chi_{\text{mol}} / M_{\text{mol}}, \quad (30)$$

where  $\rho$  is the density and  $M_{\text{mol}}$  the molar mass, the total volume susceptibility is given by

$$\chi_V^{\text{tot}} = \chi_V^{A^+} + \chi_V^e + \chi_V^A + \chi_V^{A_2^+} + \chi_V^{A_2}. \quad (31)$$

## B. Explicit expressions for the contributions to the magnetic susceptibility

Within the frame of the given model, the expanded liquid metal consists of free electrons  $e$  and ions  $A^+$ , of neutral atoms  $A$  and dimers  $A_2$ , and of molecular ions  $A_2^+$  with strongly varying concentrations along the liquid-vapor coexistence curve. All these species contribute to the magnetic susceptibility of the system so that we need the respective density- and temperature-dependent expressions.

### 1. Susceptibility of the ion cores

The first contribution in Eq. (31) is the diamagnetic susceptibility of the alkali-metal ion cores  $\text{Cs}^+$  and  $\text{Rb}^+$  which have closed electron shells. Therefore, this part is considered to be almost constant, whether or not the ions are free or bound in atoms, dimers, or molecular ions. Furthermore, it is assumed to be independent of density and temperature. Then, this contribution is simply given by  $\chi_V^{A^+} = \rho \chi_{\text{mol}}^{A^+} / M_{\text{mol}}^{A^+}$ . The densities  $\rho$  for a given temperature  $T$  were taken from the data of Jüngst, Knuth, and Hensel<sup>4</sup> for the coexistence curves of Cs and Rb. Freyland<sup>11</sup> and Warren, Brenner, and El-Hanany<sup>17</sup> used



relatively old data<sup>65</sup> for the molar susceptibilities of Cs ( $-35 \times 10^{-6} \text{ cm}^3 \text{ mol}^{-1}$ ) and Rb ( $-25 \times 10^{-6} \text{ cm}^3 \text{ mol}^{-1}$ ). Using Hartree-Fock wave functions<sup>66</sup> in Eq. (29), one finds not so different values, namely  $-40.6 \times 10^{-6} \text{ cm}^3 \text{ mol}^{-1}$  for Cs and  $-24.9 \times 10^{-6} \text{ cm}^3 \text{ mol}^{-1}$  for Rb.

## 2. Free-electron susceptibility

The contribution of free electrons consists of both paramagnetic and diamagnetic parts,  $\chi_V^e = \chi_V^{e,\text{par}} + \chi_V^{e,\text{dia}}$ . The paramagnetic susceptibility is given by the Stoner model, Eq. (22). The Lindhard function, Eq. (20), was calculated for the static case in its general form for densities and temperatures along the coexistence curve of Cs and Rb. In this way, we accounted for the gradual transition to nondegenerate conditions and the possibility of thermal excitations when approaching the critical point. The frequently used high-density limit of Eq. (20) is strictly valid only for the metal near the melting point. We have considered the local-field corrections in the form given by Ichimaru and Utsumi<sup>67</sup> which are valid for  $r_S \leq 15$ . The use of this parametrization has also led to improved data for the conductivity of Cs from the melting point up to twice the critical density.<sup>36</sup> The resulting enhancement factors and Korringa ratios for Cs and Rb

are compared in Table II with the experimental findings and a satisfactory agreement can be pointed out.

The diamagnetic part was calculated by Vignale, Rasolt, and Geldart<sup>68</sup> in the RPA. They found that the many-particle corrections have a considerably smaller effect on  $\chi_V^{e,\text{dia}}$  than on  $\chi_V^{e,\text{par}}$ . Furthermore, the diamagnetic susceptibility is decreased by the interactions and not enhanced as the paramagnetic part. The numerical results indicate an almost linear decrease with respect to  $r_S$ . The high-density expansion of Kanazawa and Matsudawa<sup>69</sup> which was often used to extract the paramagnetic susceptibility from the measured mass susceptibility, shows an opposite behavior and may be the source of (small) systematic errors in the earlier curves for the spin susceptibility as in Fig. 1.

## 3. Susceptibility of localized states

The unpaired electrons bound in atoms  $A$  and molecular ions  $A_2^+$  yield a paramagnetic susceptibility according to the Curie law, Eq. (28), with the respective partial densities instead of  $n_e$ . Furthermore, they show also orbital magnetization with a corresponding diamagnetic susceptibility according to Eq. (29). For the calculation of the expectation value  $\langle r^2 \rangle$ , we need the wave functions

TABLE II. Calculated enhancement factors of the Pauli spin susceptibility and Korringa ratios for Cs and Rb at the melting point using the local-field corrections of Ichimaru and Utsumi (Ref. 67) and the cyclotron resonance mass given by Grimes and Kip (Ref. 83) compared to experimental data and more detailed theoretical calculations.

Element	Enhancement factor	Korringa ratio	
Cs	2.336	0.412	Present calculation
	$1.76 \pm 0.06$		Knecht, <sup>a</sup> dHvA
	$2.24 \pm 0.06$		Knecht, <sup>a</sup> dHvA
	2.44		Dupree and Seymour <sup>b</sup>
	$2.14 \pm 0.01$		Springford, Templeton, and Coleridge, <sup>c</sup> dHvA
	2.20		Vosko, Perdew, and MacDonald, <sup>d</sup> theory (DFT)
		0.578	Narath and Weaver <sup>e</sup>
Rb		$0.61 \pm 0.02$	El-Hanany, Brennert, and Warren, <sup>f</sup> NMR
		0.590	Shaw and Warren, <sup>g</sup> theory (XC)
	1.703	0.627	Present calculation
	$1.724 \pm 0.008$		Knecht, <sup>a</sup> dHvA
	$1.55 \pm 0.10$		Dunifer, Pinkel, and Schulz, <sup>h</sup> spin waves.
	1.93		Dupree and Seymour <sup>b</sup>
	1.78		Vosko, Perdew, and MacDonald, <sup>d</sup> theory (DFT)
	0.617	Narath and Weaver <sup>e</sup>	
	0.628	Shaw and Warren, <sup>g</sup> theory (XC)	

<sup>a</sup>B. Knecht, *J. Low Temp. Phys.* **21**, 619 (1975); de Haas-van Alphen effect (dHvA).

<sup>b</sup>R. Dupree and E. F. W. Seymour, *Phys. Kondens. Mater* **12**, 97 (1970); see also R. Dupree and D. J. W. Geldart, *Solid State Commun.* **9**, 145 (1971).

<sup>c</sup>M. Springford, I. M. Templeton, and P. T. Coleridge, *J. Low Temp. Phys.* **53**, 563 (1983); de Haas-van Alphen effect (dHvA).

<sup>d</sup>Reference 84; density-functional theory (DFT).

<sup>e</sup>A. Narath and H. T. Weaver, *Phys. Rev.* **175**, 373 (1968).

<sup>f</sup>Reference 16; nuclear magnetic resonance (NMR).

<sup>g</sup>R. W. Shaw, Jr., and W. W. Warren, Jr., *Phys. Rev. B* **3**, 1562 (1971); exchange-correlation (XC) potential taken from R. W. Shaw, Jr., *J. Phys. C* **3**, 1140 (1970).

<sup>h</sup>G. L. Dunnifer, D. Pinkel, and S. Schulz, *Phys. Rev. B* **10**, 3159 (1974).

of the atoms, molecular ions, and also of the spin-paired dimers dependent on density.

These wave functions are tabulated in certain approximations such as the Hartree-Fock-Roothan scheme<sup>70</sup> for the isolated atoms of almost all elements. Using the quantum defect theory for the determination of  $\langle r^2 \rangle_A$  for the alkali-metal atoms [as earlier for the calculation of the quasiparticle shifts  $\Delta_e^{\text{pp}}$ , Eq. (13)] yields reasonable results compared with more detailed calculations<sup>71</sup> with deviations of less than 10%. The respective values for the valence electron contributions are for Cs  $-25 \times 10^{-6} \text{ cm}^3 \text{ mol}^{-1}$  and for Rb  $-22 \times 10^{-6} \text{ cm}^3 \text{ mol}^{-1}$ .

Considerable less information is available for the magnetic susceptibilities of isolated molecular ions  $A_2^+$  and dimers  $A_2$  (see Ref. 72). Though powerful methods such as the molecular orbital method or ingenious variational schemes have been developed for the construction of their wave functions, most of the results refer to the molecular ion and the molecule of hydrogen, to those of the lighter elements such as Li and Na, and to some simple molecules like  $\text{NH}_3$  and  $\text{CH}_4$ . If there are experimental data from molecular beam studies available, typical deviations from the calculated values are less than 10%.

Aside from the fact that there are to our knowledge no data for the diamagnetic susceptibilities of the molecular ions and dimers of Rb and Cs up to now, those data would apply only for the dilute vapor, but not for the dense vapor near the critical point where these clusters reach higher concentrations. There, the wave functions have to be solutions of respective  $N$ -particle Bethe-Salpeter equations which take into account density effects. Noting the complexity of calculating *atomic* wave functions and energy levels<sup>73</sup> even for the case of  $N=2$ , and the extensive numerical calculations necessary for the determination of the electronic structure of *isolated* higher clusters, a solution seems to be out of reach.

Therefore, we make a simple estimate for these contributions neglecting their density dependence. The wave function of the valence electron in the molecular ion  $A_2^+$  is constructed within a variational method utilizing the atomic wave functions already known from the quantum defect theory. This method will lead to smaller binding energies and to larger equilibrium distances compared with more detailed theories as we know from the study of the hydrogen molecular ion.<sup>74</sup> The resulting diamagnetic susceptibilities according to Eq. (29) should therefore be upper limits. The values for  $\text{Cs}_2^+$  and  $\text{Rb}_2^+$  are  $-47 \times 10^{-6} \text{ cm}^3 \text{ mol}^{-1}$  and  $-38.5 \times 10^{-6} \text{ cm}^3 \text{ mol}^{-1}$ , respectively.

We adopted these values also for the diamagnetic susceptibilities of the neutral dimers. Though there is orbital magnetization by two valence electrons compared to one in molecular ions, these are more strongly bonded and also the equilibrium distance is shorter in dimers. The two effects tend to compensate.

The total diamagnetic susceptibility of the dimers, the sum of the valence electron and the ionic core contributions, amounts to about  $-128 \times 10^{-6} \text{ cm}^3 \text{ mol}^{-1}$  for  $\text{Cs}_2$  and  $-88 \times 10^{-6} \text{ cm}^3 \text{ mol}^{-1}$  for  $\text{Rb}_2$  within the given model. These values seem to be reasonable in comparison, for instance, with that of the  $I_2$  molecule,  $-90 \times 10^{-6}$

$\text{cm}^3 \text{ mol}^{-1}$ .<sup>75</sup> Applying the current estimate to  $\text{Li}_2$ , a value of  $-23 \times 10^{-6} \text{ cm}^3 \text{ mol}^{-1}$  is obtained which is also in reasonable agreement with that of  $-33 \times 10^{-6} \text{ cm}^3 \text{ mol}^{-1}$  given in Ref. 76.

A further mechanism which might contribute to the total susceptibility of molecules is Van Vleck paramagnetism<sup>77</sup> which is due to virtual transitions to excited states similar to the electric polarizability. Considering the rough approximations made for the determination of the diamagnetic contributions and the relatively small Van Vleck susceptibility of  $\text{H}_2$  (less than 5% of the diamagnetic susceptibility<sup>78</sup>), we neglect these processes. However, the latter argument has to be checked when the matrix elements for these transitions are available for  $\text{Cs}_2$  and  $\text{Rb}_2$  dimers, because the respective transition energies are much smaller than in H.

Ross *et al.*<sup>79</sup> have recently performed total energy calculations for expanded solid Cs in the local density approximation and found that the diatomic form is more stable than the monoatomic form. Furthermore, energetically attractive low-lying electron excited states were predicted for  $\text{Cs}_2$ - $\text{Cs}_2$  tetramers from a molecular-orbital configuration interaction calculation. These states would be thermally populated in the expanded metal region and might contribute to the paramagnetic susceptibility dependent on their symmetry.

The stability of an electron gas to formation of bound states around a pair of ions was tested earlier by Ferraz, March, and Flores<sup>80</sup> considering Thomas-Fermi screening between the charges within the Heitler-London method for  $\text{H}_2$ . They argued that this mechanism may be responsible for the metal-nonmetal transition in dense H and gave also reasonable estimates for the corresponding critical  $r_S$  values for the alkali-metal elements by a scaling procedure.

#### IV. RESULTS FOR THE MAGNETIC PROPERTIES

We calculate the magnetic properties along the liquid-vapor coexistence curve with the data for the composition of Cs and Rb obtained in Sec. II. We will compare with values for the mass susceptibility  $\chi_g$  originally measured by Freyland.<sup>11,12</sup> Extracting the electronic, paramagnetic volume susceptibility  $\chi_V^{\text{el}}$  as shown in Fig. 1, the peculiarities of the magnetic properties are discussed with regard to the metal-nonmetal transition.

##### A. Magnetic susceptibility

The calculated magnetic mass and volume susceptibilities along the coexistence curves of Cs and Rb are shown in Figs. 3 and 4, respectively. Within the present approach, we are able to reproduce the experimental behavior for the mass susceptibility  $\chi_g$  over the whole density range from the low-density, nonmetallic vapor up to the high-density metal at the melting point. The deviations from Freyland's data do not exceed 25% for densities up to twice the critical density which is a reasonable result considering (a) the approximations made for the solution of the EOS and the calculation of the respective quasiparticle shifts and partition functions, (b) the uncertainties in determining some of the density dependent contributions to the total susceptibility, and (c) the error

bars for the experimental values, especially in the vapor, and the absence of experimental results for the region near the critical point.

For densities between two and three times the critical density, where the mass susceptibility is decreasing, our values are systematically too small. This indicates that the chemical picture of individual species as applied here becomes more and more invalid with increasing density. The behavior of the mass susceptibility in that region can also not be derived from the one-electron theories developed for solid state densities. An extended cluster model which considers large and fluctuating clusters in addition to the present model seems to be more appropriate for this region. The corresponding results for the magnetic properties of small metallic clusters in Li, Na, and K available so far<sup>81,82</sup> indicate stable localized spins in the  $A_3$  and  $A_7$  clusters.

Approaching the melting point, the enhancement of the susceptibility is described by the conventional Stoner model for the electron gas in metals (see Table II). Considering the cyclotron resonance mass as given by Grimes and Kip<sup>83</sup> for the effective electron mass together with the local-field corrections of Ichimaru and Utsumi,<sup>67</sup> the

arrows in Figs. 3 and 4 show good agreement with the experimental values for the mass and volume susceptibility. However, such an agreement is not unique and has also been achieved with other combinations of these parameters (see Ref. 60). The density-functional formalism developed by Vosko and co-workers<sup>84</sup> yields the best enhancement factors at the melting point for all alkali metals compared to the experimental values.

Furthermore, we have displayed the electronic paramagnetic susceptibility per volume  $\chi_V^{e,par}$ . We compare with the previous results which were extracted from the experimental data by subtracting the diamagnetic contributions of the simple ions and the conduction electrons (see Fig. 1). The Curie law for one electron per atom is considered to yield an upper limit for the paramagnetic susceptibility.

The experimentally observed deviations from the Curie law at vapor densities are clearly a result of the formation of spin-paired dimers in that region as already pointed out by Freyland.<sup>11,12</sup> He extracted dimer fractions for Cs and Rb by applying simple mass action laws to his data without considering nonideality corrections similar to our values in the dilute vapor. Hohl<sup>85</sup> has given recently

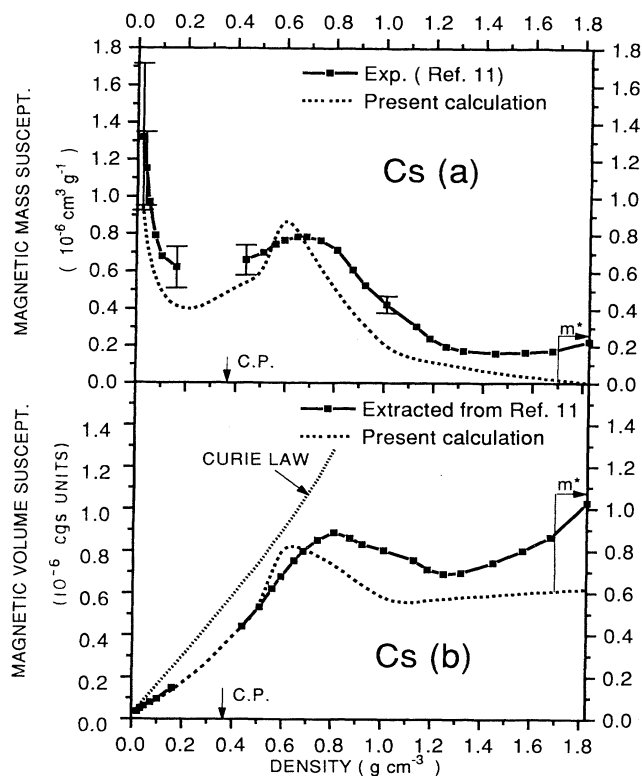


FIG. 3. Total magnetic mass (a) and electronic, paramagnetic volume susceptibility (b) of Cs along the liquid-gas coexistence curve. Continuous line: experimental values of Ref. 11 (solid squares). Short broken line: present calculation. Short dotted line: Curie law for one electron per atom. Critical point (CP) indicated by arrow. Taking into account the effective mass  $m^*$  of Ref. 83 at the melting point yields values indicated by arrows which are in reasonable agreement with the measured susceptibilities (see Table II).

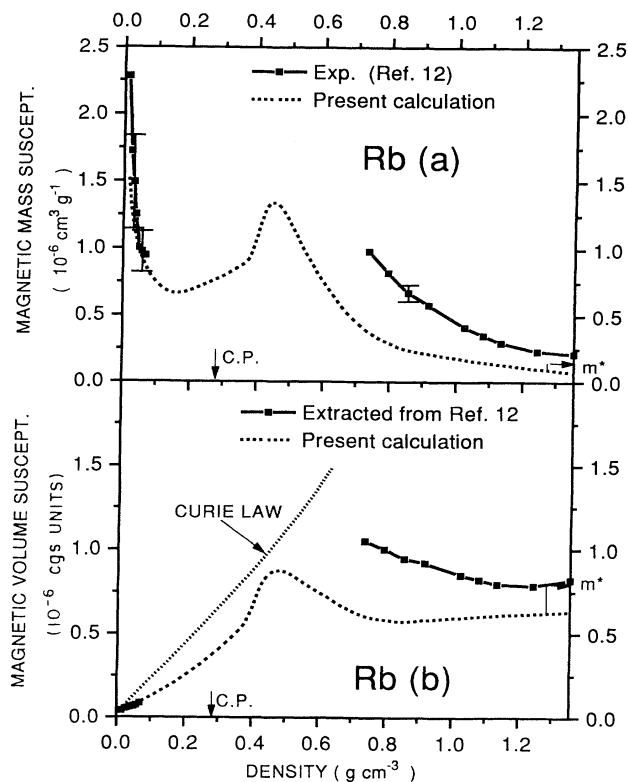


FIG. 4. Total magnetic mass (a) and electronic, paramagnetic volume susceptibility (b) of Rb along liquid-gas coexistence curve. Continuous line: experimental values of Ref. 12 (solid squares). Short broken line: present calculation. Short dotted line: Curie law for one electron per atom. Critical point (CP) indicated by arrow. Taking into account the effective mass  $m^*$  of Ref. 83 at the melting point yields values indicated by arrows which are in reasonable agreement with the measured susceptibilities (see Table II).

analogous estimates for Cs, Rb, and K based on new experimental data for the EOS.<sup>4,5</sup> The deformation of the Curie curve can thus serve as a measure for the amount of spin-paired species in the system.

The enhancement of the electronic paramagnetic susceptibility at about twice the critical density can be explained in our model by the formation of molecular ions  $A_2^+$  which give a Curie-like contribution due to their localized electrons. This peak in the susceptibility-density plot for Cs was interpreted by Chapman and March<sup>86</sup> as the limitation of enhanced Pauli paramagnetism and a consequent crossover to a Curie-like regime. They treated a correlation-induced metal-nonmetal transition in expanded fluid alkali metals phenomenologically by a finite temperature extension of the theory of Brinkman and Rice.<sup>21</sup> At this special point,  $\rho \approx 0.8 \text{ g cm}^{-3}$  and  $T \approx 1780 \text{ K}$ , they found a ratio  $k_B T/E_F \approx 0.18$  from the renormalization of the electron degeneracy temperature due to the effects of correlation. Taking the fraction of free electrons from our composition data [see Fig. 2(a)] we find a very similar value of 0.25. As the molecular ions vanish with increasing density, a susceptibility minimum occurs at about three times the critical density.

The results for the paramagnetic susceptibility between two and three times the critical density may change when higher clusters are taken into account as proposed above for the improvement of the data for the mass susceptibility. Although chemically stable higher clusters such as  $A_3$  or  $A_3^+$  are of less importance within our model, fluctuating charged and neutral clusters may develop in that region at elevated temperatures. A phenomenological model for those fluctuating clusters was utilized by Likalter<sup>87</sup> in order to explain the behavior of the electrical conductivity in the region of the metal-nonmetal transition.

The decrease of the electronic paramagnetic susceptibility in the liquid metal range from the melting point down to three times the critical density seems to be a consequence of a reduced effective electron mass. This assumption is supported by the one-electron band structure calculations mentioned earlier,<sup>21,22</sup> where a reduced density of states at the Fermi level was found for various crystal structures simulating the decreasing coordination number during the expansion of the liquid.

### B. Korringa relation

Though the consideration of bound states leads to a reasonable overall agreement between the calculated and measured susceptibilities, the experimentally observed behavior of the Korringa ratio  $\eta$  cannot be explained within our model.

For the normal liquid metal domain, the Korringa ratio  $\eta_{ST}$  is recovered from the one-particle contribution  $\chi^{(1)}$  to the total susceptibility and a reasonable agreement with the experimental value can be pointed out (see Table II).

In the expanded metal domain, a decrease is obtained for the Korringa ratio from the Stoner model which is in contrast to the experimental findings.<sup>17</sup> This failure is not removed by the two-particle contribution  $\chi^{(2)}$ . In

fact the decrease becomes more pronounced. Because the scaling of the nuclear relaxation rate with the Knight shift as expressed by the Korringa relation does not apply for localized spins, this result is not surprising.

We conclude that the current approximations for the polarization function are not sufficient for the explanation of the behavior of the Korringa ratio in the expanded metal. Warren, Brennert, and El-Harany<sup>17</sup> have developed a semiquantitative description of the Korringa ratio behavior in terms of enhancement of the dynamic, nonuniform susceptibility. From this point of view, the observed increase in the Korringa ratio at low density is seen to reflect a change in the character of electron spin fluctuations from ferromagnetic enhancement in the normal metal to antiferromagnetic enhancement in the expanded metal. In terms of the present description, the development of antiferromagnetic spin fluctuation character corresponds to formation of  $Cs_2$  dimers and other spin-paired clusters. A similar phenomena in low-dimensional solids is the well-known Peierls distortion. The physics may be the same in both cases, i.e., a lowering of the electronic energy by formation of the spin-paired bound state which more than compensates an increase in the ion-ion repulsion (elastic energy in the solid).

### C. Charge density at the nucleus

The charge density at the nucleus,  $\langle |\Psi(0)|^2 \rangle_F$ , averaged at the Fermi level, can be extracted from the NMR and susceptibility measurements. Comparing the Cs results with the atomic value of  $|\Psi(0)|_a^2 = 2.58 \times 10^{25} \text{ cm}^{-3}$ ,<sup>88</sup> Warren, Brennert, and El-Harany<sup>17</sup> found a ratio of  $\xi \approx \frac{1}{2}$  for the normal liquid metal at high densities. Below three times the critical density, the ratio is decreasing markedly while, after reaching a minimum value of about 0.28 at twice the critical density, it starts to increase. The value 1 has to be approached in the low-density vapor. They have pointed out that this behavior cannot be due to spin pairing in dimers because these particles do not contribute to the paramagnetic susceptibility.

ESR studies of neutral Li, Na, and K clusters<sup>89</sup> have shown a diminishing  $s$  character with increasing cluster size. The ratio  $\xi$  decreases monotonically from the atomic value 1 towards the respective value in bulk metal and shows no sign of a minimum behavior. The band structure calculations for the expanded liquid<sup>21,22</sup> also yield a simple monotonic increase towards the atomic value and fail to account a decrease of this quantity.

A displacement of charge density away from the ion cores does occur in molecular ions in the expanded metal. The charge density in  $H_2^+$ , for instance, reaches about 40% of the value in atomic H. Using the same wave functions as for the determination of the diamagnetic susceptibilities, the respective values are 47% for  $Cs_2^+$  and 46% for  $Rb_2^+$  which yield a strong decrease of the ratio  $\xi$ , but not the minimum for  $\xi \sim 0.25$  as found experimentally. A further drastic decrease would appear if excited electronic states of charged and neutral clusters reach considerable concentrations, and if fluctuating clusters develop at elevated temperatures.

## V. CONCLUSIONS

We have calculated the magnetic mass and volume susceptibility along the coexistence curves of Cs and Rb and were able to explain the experimental behavior of the mass susceptibility  $\chi_g$  over the whole density range from the low-density, nonmetallic vapor up to the high-density metal at the melting point.

The composition of Cs and Rb was determined by means of a quantum statistical EOS originally derived for partially ionized plasmas which takes into account the interaction corrections between the various species in a systematic way. An approximate self-consistent solution for the system of coupled mass action laws describes the formation of atoms  $A$ , dimers  $A_2$ , and molecular ions  $A_2^+$  out of the elementary particles electrons  $e$  and simple ions  $A^+$ .

The paramagnetic and diamagnetic contributions of these species to the total susceptibility are, in general, density and temperature dependent. We have used standard results for these quantities. The paramagnetic (Pauli) susceptibility of free electrons was calculated on an extended RPA level utilizing the local-field corrections of Ichimaru and Utsumi.<sup>67</sup> Taking into account the effective electron mass,<sup>83</sup> the conventional Stoner model for the enhancement of the susceptibility in the normal metal is recovered. Reasonable agreement is achieved for the enhancement parameter as well as for the Korringa ratio of Cs and Rb at the melting point (see Table II).

For the diamagnetic (Landau) susceptibility of free electrons we have inserted the numerical RPA results of Vignale, Rasolt, and Geldart.<sup>68</sup> The earlier results of Kanazawa and Matsudawa<sup>69</sup> which were frequently used to extract the paramagnetic part out of the total susceptibility are valid only in the high density limit  $r_s \rightarrow 0$  and give rise for (small) systematic errors for metal or expanded liquid densities.

Localized spins in bound states yield both paramagnetic and diamagnetic contributions to the total susceptibility. Atoms  $A$  and molecular ions  $A_2^+$  with one unpaired spin have strong Curie-like contributions, whereas spin-paired dimers can only have a Van Vleck-type paramagnetism. The latter was neglected in this paper. The diamagnetic (Langevin) terms were calculated by means of the respective wave functions [see Eq. (29)]. We have made simple approximations when rigorous results were not available, especially for the higher clusters  $A_2$  and  $A_2^+$ , which lead to upper limits for these diamagnetic terms.

The deviations of the paramagnetic susceptibility from the Curie law at vapor densities are clearly due to the formation of spin-paired dimers  $A_2$ , as pointed out already by Freyland<sup>11,12</sup> in his experimental papers, and recently by Hohl.<sup>85</sup> The maximum of the paramagnetic susceptibility at about two times the critical density is explainable in our model by the drastic increase of the fraction of molecular ions  $A_2^+$ . Both features support the applicability of the concept of cluster formation for the alkali-metal elements when increasing the density from the vapor to the expanded liquid domain. This model has already lead earlier to reasonable results for the thermo-

dynamic<sup>34,35</sup> and transport properties<sup>36,37</sup> of alkali-metal plasmas and liquids (see also Refs. 39 and 40).

A modified cluster model which considers large and fluctuating clusters in addition to the present model seems to be more appropriate for the region between two and three times the critical density, where our values are too small systematically. This seems to be an ideal subject for the concepts of cluster physics which are considered to bridge the gap between the molecular domain with its well defined individual properties and the condensed matter domain where the collective behavior dominates the physical properties.

The metal-nonmetal transition occurs in that domain where neutral and charged clusters, and eventually also higher fluctuating clusters, are formed. Such a picture coincides with the recent reverse Monte Carlo calculation of Nield, Howe, and McGreevy<sup>90</sup> who treated the metal-nonmetal transition as a bond percolation problem. They found that some finite atomic clusters are present close to the critical point as well as weak links within infinite clusters.

These ideas are strongly supported by the recent results of Ross *et al.*<sup>79</sup> for the metal-nonmetal transition in Cs. The formation of excited neutral clusters at elevated temperatures in the dense vapor is very likely to occur as one can conclude from their total energy calculations for the Cs<sub>2</sub>-Cs<sub>2</sub> cluster. The respective extra paramagnetic contributions of the excited states and the Van Vleck term of the ground state would diminish the present diamagnetic deviations from the experimental susceptibilities in the vapor and the expanded liquid.

Furthermore, the consideration of excited states of higher chemically stable clusters or fluctuating clusters would also lead to a drastic decrease of the charge density at the nucleus in this density region as it was experimentally deduced from NMR measurements.<sup>16,17</sup> The corresponding excitation mechanisms should be reflected in the imaginary part of  $\chi(\mathbf{q}, \omega)$  so that the simultaneous increase of the Korringa ratio may be derived. Neither feature is explainable by considering only the ground states of the smallest clusters as in our present model.

The consideration of electron correlations beyond the RPA level is found to be essential. The aspects of disorder which were not considered here have to be treated on the same footing.

## ACKNOWLEDGMENTS

One of the authors (R.R.) would like to thank the Physics Department, Oregon State University, for its hospitality and support during the period in which this work was performed. It is our pleasure to express our gratitude to F. Hensel for many stimulating discussions, the continuing interest in this work, and for sending us detailed data of his group's experimental results. We would like to thank M. Ross for valuable discussions and for sending us his results (Ref. 79) prior to publication. We are indebted to G. Röpke, H. J. F. Jansen, and R. Dupree for valuable discussions and comments. This work was partially supported (R.R.) by the Alexander von Humboldt Foundation, Feodor Lynen Program.

- \*On leave from the University of Rostock, Department of Physics, Universitätsplatz 1, D-18051 Rostock, Germany.
- <sup>1</sup>H. Renkert, F. Hensel, and E. U. Franck, *Ber. Bunsenges. Phys. Chem.* **75**, 507 (1971); H. P. Pfeifer, W. Freyland, and F. Hensel, *ibid.* **80**, 716 (1976); **83**, 204 (1979).
  - <sup>2</sup>G. Franz, W. Freyland, and F. Hensel, *J. Phys. (Paris) Colloq.* **41**, C8-70 (1980).
  - <sup>3</sup>F. Noll, W.-C. Pilgrim, and R. Winter, *Z. Phys. Chem. Neue Folge* **156**, 303 (1988).
  - <sup>4</sup>S. Jüngst, B. Knuth, and F. Hensel, *Phys. Rev. Lett.* **55**, 2160 (1985).
  - <sup>5</sup>F. Hensel, M. Stolz, G. Hohl, R. Winter, and W. Götzlaff, *J. Phys. IV (Paris) Colloq.* **1**, C5-191 (1991).
  - <sup>6</sup>J. Cook, *Can. J. Phys.* **59**, 25 (1981); **60**, 1311 (1982); **60**, 1759 (1982).
  - <sup>7</sup>W. Götzlaff, G. Schönherr, and F. Hensel, *Z. Phys. Chem. Neue Folge* **156**, 219 (1988).
  - <sup>8</sup>R. Winter, F. Hensel, T. Bodensteiner, and W. Gläser, *Ber. Bunsenges. Phys. Chem.* **91**, 1327 (1987); R. Winter and F. Hensel, *Phys. Chem. Liq.* **20**, 1 (1989).
  - <sup>9</sup>R. Winter, W.-C. Pilgrim, and F. Hensel, *J. Phys. IV (Paris) Colloq.* **1**, C5-45 (1991).
  - <sup>10</sup>H. Uchtmann, U. Brusius, M. Yao, and F. Hensel, *Z. Phys. Chem. Neue Folge* **156**, 151 (1988).
  - <sup>11</sup>W. Freyland, *Phys. Rev. B* **20**, 5104 (1979).
  - <sup>12</sup>W. Freyland, *J. Phys. (Paris) Colloq.* **41**, C8-74 (1980).
  - <sup>13</sup>L. Bottyan, R. Dupree, and W. Freyland, *J. Phys. F* **13**, L173 (1983).
  - <sup>14</sup>C. van der Marel, P. Heitjans, B. Bader, P. Freiländer, A. Schirmer, and W. Freyland, *Z. Phys. Chem. Neue Folge* **157**, 593 (1988).
  - <sup>15</sup>W. W. Warren, Jr., *Phys. Rev. B* **29**, 7012 (1984).
  - <sup>16</sup>U. El-Hanany, G. F. Brennert, and W. W. Warren, Jr., *Phys. Rev. Lett.* **50**, 540 (1983).
  - <sup>17</sup>W. W. Warren, Jr., G. F. Brennert, and U. El-Hanany, *Phys. Rev. B* **39**, 4038 (1989).
  - <sup>18</sup>For reviews, see D. Pines and P. Nozieres, *The Theory of Quantum Liquids* (Addison-Wesley, Redwood City, 1989); R. M. White, *Quantum Theory of Magnetism* (Springer, Berlin, 1983); J. Winter, *Magnetic Resonance in Metals* (Clarendon, Oxford, 1971).
  - <sup>19</sup>For reviews, see K. S. Singwi and M. P. Tosi, in *Solid State Physics: Advances in Research and Applications*, edited by H. Ehrenreich, F. Seitz, and D. Turnbull (Academic, New York, 1981), Vol. 36, p. 177; S. Ichimaru, *Rev. Mod. Phys.* **54**, 1017 (1982); S. Ichimaru, S. Mitake, S. Tanaka, and X.-Z. Yan, *Phys. Rev. A* **32**, 1768 (1985); S. Mitake, S. Tanaka, X.-Z. Yan, and S. Ichimaru, *ibid.* **32**, 1775 (1985).
  - <sup>20</sup>For reviews, see N. F. Mott and E. A. Davis, *Electronic Processes in Non-Crystalline Materials* (Clarendon, Oxford, 1971); N. F. Mott, *Metal-Insulator Transitions* (Taylor and Francis, London, 1974).
  - <sup>21</sup>W. F. Brinkman and T. M. Rice, *Phys. Rev. B* **2**, 4302 (1970).
  - <sup>22</sup>W. W. Warren, Jr. and L. F. Mattheiss, *Phys. Rev. B* **30**, 3103 (1984).
  - <sup>23</sup>P. J. Kelly and D. Glötzel, *Phys. Rev. B* **33**, 5284 (1986).
  - <sup>24</sup>L. M. Sander, H. B. Shore, and J. H. Rose, *Phys. Rev. B* **24**, 4879 (1981); B. I. Min, T. Oguchi, H. J. F. Jansen, and A. J. Freeman, *ibid.* **33**, 324 (1986).
  - <sup>25</sup>P. W. Anderson, *Phys. Rev.* **109**, 1492 (1958).
  - <sup>26</sup>D. E. Logan, *J. Chem. Phys.* **94**, 628 (1991).
  - <sup>27</sup>S. Ichimaru, *Plasma Physics* (Benjamin, Menlo Park, CA, 1986).
  - <sup>28</sup>W. Ebeling, W.-D. Kraeft, and D. Kremp, *Theory of Bound States and Ionization Equilibrium in Plasmas and Solids* (Akademie-Verlag, Berlin, 1976).
  - <sup>29</sup>V. K. Gryaznov *et al.*, *Thermophysical Properties of the Working Media of Gas-Phase Nuclear Reactor* (Atomizdat, Moscow, 1980), in Russian.
  - <sup>30</sup>W.-D. Kraeft, D. Kremp, W. Ebeling, and G. Röpke, *Quantum Statistics of Charged Particle Systems* (Akademie-Verlag, Berlin, 1986).
  - <sup>31</sup>For Xe, see, for example, W. Ebeling, A. Förster, W. Richert, and H. Hess, *Physica A* **150**, 159 (1988).
  - <sup>32</sup>For H, see, for example, D. Saumon and G. Chabrier, *Phys. Rev. A* **46**, 2084 (1992), and references therein.
  - <sup>33</sup>The latest results on the plasma phase transition are summarized in the *Proceedings of the International Conference on the Physics of Strongly Coupled Plasmas*, edited by H. M. Van Horn and S. Ichimaru (Rochester University Press, New York, 1993).
  - <sup>34</sup>R. Redmer and G. Röpke, *Physica A* **130**, 523 (1985); R. Redmer, T. Rother, K. Schmidt, W.-D. Kraeft, and G. Röpke, *Contrib. Plasma Phys.* **28**, 41 (1988).
  - <sup>35</sup>R. Redmer and G. Röpke, *Contrib. Plasma Phys.* **29**, 343 (1989).
  - <sup>36</sup>R. Redmer, H. Reinholz, G. Röpke, R. Winter, F. Noll, and F. Hensel, *J. Phys. Condens. Matter* **4**, 1659 (1992).
  - <sup>37</sup>H. Reinholz and R. Redmer, *J. Non-Cryst. Solids* **156-158**, 654 (1993).
  - <sup>38</sup>F. E. Höhne, R. Redmer, G. Röpke, and H. Wegener, *Physica A* **128**, 643 (1984).
  - <sup>39</sup>V. A. Alekseev and I. T. Iakubov, *Phys. Rep.* **96**, 1 (1983). Cluster models have been applied for the calculation of the electrical conductivity of partially ionized alkali-metal plasmas by V. V. Gogoleva, V. Yu. Zitserman, A. Ya. Polishchuk, and I. T. Iakubov, *Teplofiz. Vys. Temp.* **22**, 208 (1984); and N. N. Iermohin, B. M. Kovaliov, P. P. Kulik, and V. A. Riabii, *J. Phys. (Paris) Colloq.* **39**, C1-200 (1978).
  - <sup>40</sup>J. P. Hernandez, *Phys. Rev. Lett.* **53**, 2320 (1984); *Phys. Rev. A* **31**, 932 (1985); *Phys. Rev. Lett.* **57**, 3183 (1986); *Phys. Rev. A* **34**, 1316 (1986).
  - <sup>41</sup>L. P. Kadanoff and G. Baym, *Quantum Statistical Mechanics* (Benjamin, New York, 1962).
  - <sup>42</sup>H. Stolz and R. Zimmermann, *Phys. Status Solidi B* **94**, 135 (1979).
  - <sup>43</sup>D. Kremp, M. K. Kilimann, W.-D. Kraeft, H. Stolz, and R. Zimmermann, *Physica A* **127**, 646 (1984).
  - <sup>44</sup>G. Röpke, L. Münchow, and H. Schulz, *Nucl. Phys. A* **379**, 526 (1982); G. Röpke, M. Schmidt, L. Münchow, and H. Schulz, *ibid.* **399**, 587 (1983); G. Röpke, M. Schmidt, and H. Schulz, *ibid.* **424**, 594 (1984).
  - <sup>45</sup>D. Kremp, W.-D. Kraeft, and A. J. D. Lambert, *Physica A* **127**, 72 (1984).
  - <sup>46</sup>R. Zimmermann and H. Stolz, *Phys. Status Solidi B* **131**, 151 (1985).
  - <sup>47</sup>G. E. Beth and E. Uhlenbeck, *Physica (Utrecht)* **3**, 729 (1936); **4**, 915 (1937).
  - <sup>48</sup>D. Bollé, *Ann. Phys. (N.Y.)* **121**, 131 (1979); see also his contribution in *Strongly Coupled Plasma Physics*, edited by F. J. Rogers and H. E. DeWitt (Plenum, New York, 1987), p. 215.
  - <sup>49</sup>F. J. Rogers, *Astrophys. J.* **310**, 723 (1986); see also his contribution in *Strongly Coupled Plasma Physics*, edited by F. J. Rogers and H. E. DeWitt (Plenum, New York, 1987), p. 261.
  - <sup>50</sup>W. Ebeling and W. Richert, *Ann. Phys. (Leipzig)* **39**, 362 (1982); see also *Phys. Status Solidi B* **128**, 467 (1985); *Phys. Lett. A* **108**, 80 (1984).
  - <sup>51</sup>M. Gell-Mann and K. A. Brueckner, *Phys. Rev.* **106**, 364

- (1957).
- <sup>52</sup>W. Ebeling and H. Lehmann, *Ann. Phys. (Leipzig)* **45**, 529 (1988); see also S. Tanaka, S. Mitake, X.-Z. Yan, and S. Ichimaru, *Phys. Rev. A* **32**, 1779 (1985).
- <sup>53</sup>R. Redmer, G. Röpke, and R. Zimmermann, *J. Phys. B* **20**, 4069 (1987). For the quantum defect theory, see A. Burgess and M. J. Seaton, *Mon. Not. R. Astron. Soc.* **120**, 121 (1960).
- <sup>54</sup>R. Redmer (unpublished).
- <sup>55</sup>G. A. Mansoori, N. F. Carnahan, K. E. Starling, and T. W. Leland, *J. Chem. Phys.* **54**, 1523 (1971); see also W. Ebeling and K. Scherwinski, *Z. Phys. Chem. (Leipzig)* **264**, 1 (1983).
- <sup>56</sup>See, for example, K. P. Huber and G. Herzberg, *Molecular Spectra and Molecular Structure, Vol. IV.: Constants of Diatomic Molecules* (Van Nostrand, New York, 1979).
- <sup>57</sup>T. H. Miller and B. Bederson, *Adv. At. Mol. Phys.* **13**, 1 (1977).
- <sup>58</sup>F. London, *Z. Phys. Chem.* **11**, 222 (1930).
- <sup>59</sup>J. Lindhard, K. Dan. Vidensk., Selsk. Mat. Fys. Medd. **8**, 1 (1954).
- <sup>60</sup>T. Kushida, J.C. Murphy, and M. Hanabusa, *Phys. Rev. B* **13**, 5136 (1976). We refer especially to Fig. 6 of that paper, where the variety of the theoretical predictions for the susceptibility enhancement due to local-field corrections is shown.
- <sup>61</sup>N. Iwamoto and D. Pines, *Phys. Rev. B* **29**, 3924 (1984); N. Iwamoto, E. Krotscheck, and D. Pines, *ibid.* **29**, 3936 (1984).
- <sup>62</sup>T. Moriya, *J. Phys. Soc. Jpn.* **18**, 516 (1963).
- <sup>63</sup>P. Bhattacharyya, K. N. Pathak, and K. S. Singwi, *Phys. Rev. B* **3**, 1568 (1971).
- <sup>64</sup>G. Röpke and R. Der, *Phys. Status Solidi B* **92**, 501 (1979). For a more detailed discussion, see Chap. 4.5. of Ref. 30.
- <sup>65</sup>G. W. Brindley and F. E. Hoare, *Trans. Faraday Soc.* **33**, 268 (1937); *Proc. Phys. Soc. London* **49**, 619 (1937).
- <sup>66</sup>W. R. Johnson, D. Kolb, and K.-N. Huang, *At. Data Nucl. Data Tables* **28**, 333 (1983).
- <sup>67</sup>S. Ichimaru and K. Utsumi, *Phys. Rev. B* **24**, 7385 (1981); see also K. Utsumi and S. Ichimaru, *ibid.* **22**, 1522 (1980); **22**, 5203 (1980).
- <sup>68</sup>G. Vignale, M. Rasolt, and D. J. W. Geldart, *Phys. Rev. B* **37**, 2502 (1988).
- <sup>69</sup>H. Kanazawa and N. Matsudawa, *Prog. Theor. Phys.* **23**, 433 (1960).
- <sup>70</sup>E. Clementi and C. Roetti, *At. Data Nucl. Data Tables* **14**, 177 (1974).
- <sup>71</sup>For the calculation of accurate binding energies, polarizabilities, and susceptibilities for the alkali-metal atoms  $A$ , the dissociation energies, equilibrium distances, rotational constants, and vibration frequencies of the alkali-metal molecular ions  $A_2^+$  and dimers  $A_2$ , see (a) W. Müller, J. Flesch, and W. Meyer, *J. Chem. Phys.* **80**, 3297 (1984); (b) W. Müller and W. Meyer, *ibid.* **80**, 3311 (1984); (c) L. von Szentpaly, *Chem. Phys. Lett.* **88**, 321 (1982); (d) J. Flad, G. Igel, M. Dolg, H. Stoll, and H. Preuss, *Chem. Phys.* **75**, 331 (1983).
- <sup>72</sup>Molecular orbitals for the dimers from  $H_2$  to  $Ar_2$  were tabulated by P. E. Cade and A. C. Wahl, *At. Data Nucl. Data Tables* **13**, 339 (1981). For more general information on the magnetic properties of molecules, see, for example, D. W. Davis, *The Theory of the Electric and Magnetic Properties of Molecules* (Wiley, London, 1967), pp. 95–125; R. Ditchfield, in *Physical Chemistry Series One. Volume 2: Molecular Structure and Properties*, edited by G. Allen (Butterworths, London, 1972), pp. 91–157; W. G. Richards and D. L. Cooper, *Ab initio Molecular Orbital Calculations for Chemists* (Clarendon, Oxford, 1983).
- <sup>73</sup>A solution of the Bethe-Salpeter equation for the hydrogen atom was performed by R. Zimmermann, K. Kilimann, W.-D. Kraeft, D. Kremp, and G. Röpke, *Phys. Status Solidi B* **90**, 175 (1978), and recently by W.-D. Kraeft, D. Kremp, K. Kilimann, and H. E. DeWitt, *Phys. Rev. A* **42**, 2340 (1990), taking into account many-particle effects such as dynamic screening or the Pauli exclusion principle.
- <sup>74</sup>See, for example, B. H. Bransden and C. J. Joachain, *Physics of Atoms and Molecules* (Longman, London, 1983), Chap. 9.4.
- <sup>75</sup>A. Weiss and H. Witte, *Magnetochemie* (Verlag Chemie, 1973); and *Handbook of Chemistry and Physics* (Chemical Rubber, Cleveland, 1973).
- <sup>76</sup>M. Karplus and H. J. Kolker, *J. Chem. Phys.* **38**, 1263 (1963).
- <sup>77</sup>J. H. Van Vleck, *Electric and Magnetic Susceptibilities* (Cambridge University Press, Oxford, 1932).
- <sup>78</sup>J. Tillieu, *Ann. Phys. (Paris)* **2**, 471 (1957); **2**, 631 (1957).
- <sup>79</sup>M. Ross, L. Yang, B. Dahling, and N. Winter, *Z. Phys. Chemie Neue Folge* (to be published).
- <sup>80</sup>A. Ferraz, N. H. March, and F. Florres, *J. Phys. Chem. Solids* **45**, 627 (1984).
- <sup>81</sup>For a review, see *Physics and Chemistry of Small Clusters*, Vol. 158 of *NATO Advanced Study Institute, Series B: Physics*, edited by P. Jena, B. K. Rao, and S. N. Khanna (Plenum, New York, 1987). We refer especially to the contribution of W. Weltner, Jr., and R. J. Van Zee, p. 352, and references therein. See also B. K. Rao, S. N. Khanna, and P. Jena, in *Phase Transitions* (Gordon and Breach, London, 1990), Vols. 24–26, p. 35.
- <sup>82</sup>Extended calculations for the electronic structure of small Na clusters were performed by, e.g., J. L. Martins, J. Buttet, and R. Car, *Phys. Rev. B* **31**, 1804 (1985).
- <sup>83</sup>C. C. Grimes and A. F. Kip, *Phys. Rev.* **132**, 1991 (1963). Their values for the cyclotron resonance mass are 1.44 (Cs) and 1.20 (Rb). The band-structure effective masses given by F. S. Ham, *Phys. Rev.* **128**, 2524 (1962), are 1.76 (Cs) and 1.21 (Rb).
- <sup>84</sup>S. H. Vosko, J. P. Perdew, and A. H. MacDonald, *Phys. Rev. Lett.* **25**, 1725 (1975); A. H. MacDonald, J. P. Perdew, and S. H. Vosko, *Solid State Commun.* **18**, 85 (1976).
- <sup>85</sup>G. Hohl, Ph.D. thesis, Philipps-Universität Marburg, 1992.
- <sup>86</sup>R. G. Chapman and N. H. March, *Phys. Rev. B* **38**, 792 (1988).
- <sup>87</sup>A. A. Likalter, *Teplofiz. Vys. Temp.* **20**, 1076 (1982); **22**, 258 (1984).
- <sup>88</sup>P. Kusch and H. Taub, *Phys. Rev.* **75**, 1477 (1949).
- <sup>89</sup>D. A. Garland and D. M. Lindsey, *J. Chem. Phys.* **78**, 2813 (1983).
- <sup>90</sup>V. M. Nield, M. A. Howe, and R. L. McGreevy, *J. Phys. Condens. Matter* **3**, 7519 (1991).